Rational Synthesis of Antiaromatic 5,15-Dioxaporphyrin and Oxidation into β,β-Linked Dimers

Nishiyama, Akihide
Department of Chemistry and Biochemistry Graduate School of Engineering Kyushu University

Fukuda, Masaya
Department of Chemistry and Biochemistry Graduate School of Engineering Kyushu University

Mori, Shigeki
Advanced Research Support Center (ADRES) Ehime University

Furukawa, Ko
Center for Instrumental Analysis Institute for Research Promotion Niigata University

他

出版情報：Angewandte Chemie International Edition. 57 (31), pp.9728-9733, 2018-07-23. Wiley
バージョン：

COMMUNICATION

First Rational Synthesis of Antiaromatic 5,15-Dioxaporphyrin and Its β,β-Linked Dimer Formation upon Oxidation

Akihide Nishiyama, Masaya Fukuda, Shigeki Mori, Ko Furukawa, Heike Fliegl, Hiroyuki Furuta,* and Soji Shimizu**

Abstract: 5,15-Dioxaporphyrin was synthesized for the first time by a nucleophilic aromatic substitution reaction of a nickel bis(α,α'-dibromodipyrrin) complex with benzaldoxime, followed by an intramolecular annulation of the α-hydroxy-substituted intermediate. This unprecedented molecule is 20π-electron antiaromatic in terms of Hückel's rule of aromaticity because lone pair electrons of oxygen atoms are incorporated into the 18π-electron conjugated system of porphyrin. A theoretical analysis based on the gauge including magnetically induced current method confirmed its antiaromaticity and a dominant inner pathway for the ring current. Unique reactivity of 5,15-dioxaporphyrin forming a β,β-linked dimer upon oxidation was also revealed.

Porphyrin, a structure of which can be found in nature as chlorophyll of plants for light harvesting and photo-energy transfer and as heme of mammalian blood for oxygen transportation, is a naturally occurring aromatic macrocycle consisting of alternately arranged four pyrrole rings and four methine carbon atoms.[1] It is known that during the heme catabolism, heme is oxidized to verdoheme, an iron complex of 5-oxaporphyrin, in which one of the *meso*-carbon atoms is replaced by an oxygen atom, and further oxidized to biliverdin, an open-chain tetrapyrrole derivative, along with elimination of carbon monoxide and iron.[2] Stimulated by the interest in these natural porphyrin derivatives and intermediate metabolites, synthetic chemistry of porphyrin analogues bearing heteroatoms, such as nitrogen, oxygen and sulfur, at the pyrrole-bridging *meso*-positions has been intensively investigated from the early stage of porphyrin chemistry.[3] Due to the presence of the heteroatoms in the 18π-electron conjugation circuit of porphyrin, *meso*-heteroatom-substituted porphyrin analogues exhibit different optical and electrochemical properties as well as coordination abilities from those of regular porphyrins.[4] One of the representative example of hetero-atom-containing porphyrin analogues is phthalocyanine,[5] a totally *meso*-nitrogen-substituted counterpart of porphyrin, which exhibits a completely different blue color compared to the red color of porphyrin. The origin of these different colors lies in the lifted degeneracy of the HOMO by substitution of the *meso*-carbon atoms by more electronegative nitrogen atoms, which causes intensification of the Q-band absorption of phthalocyanine in the red region due to the smaller configurational interactions of transitions between the four frontier orbitals.[6] In addition to the perturbation of the 18π-electron conjugated system, heteroatom-substitution can also change the number of π-electrons involved in the main conjugation pathway. It is, therefore, conceivable that in the case of modification with two chalcogen atoms, lone-pair electrons can be included to provide antiaromatic 20π-electron conjugated systems. Despite this expectation, such kind of antiaromatic di-chalcogen-substituted porphyrin analogues have not yet been realized: 5,15-dithiaporphyrin synthesized by Johnson in 1970[7] and more recently by Shinokubo[8] is nonaromatic, whereas 5,15-dioxaporphyrin has not been synthesized. Shinokubo *et al*. ascribed the nonaromaticity of 5,15-dithiaporphyrin to its gable structure caused by the long C–S bonds, which hindered effective overlap of π-orbitals. Very recently, Matano and Shinokubo independently reported 20π-antiaromatic 5,15-diaza-5,15-dihydroporphyrin.[9,10] Considering the fact that the lone-pair electrons of amino-nitrogen atoms are successfully incorporated into the conjugated system of porphyrin, it can be anticipated that isoelectronic 5,15-dioxaporphyrin may attain a global antiaromatic π-conjugation. In addition, this kind of approach towards antiaromatic systems based on modification of main group element at the *meso*-positions is practically important although a number of stable antiaromatic molecules have successfully been created by utilizing porphyrinoid π-conjugated systems like isophlorine,[11-18] norcorrole,[19-21] and expanded porphyrins.[22,23]

We report, herein, the first rational synthesis of 5,15-dioxaporphyrin by a nucleophilic substitution reaction of a nickel bis(dipyrrin) complex with benzaldoxime followed by annulation reaction of the α-hydroxy-substituted intermediate. In clear contrast to the nonaromaticity of its higher congener, 5,15-dithiaporphyrin,[7,8] 5,15-dioxaporphyrin exhibited unequivocal antiaromatic characteristics, such as a paratropic ring current effect and a broad absorption in the visible and near infrared (Vis/NIR) regions reflecting a forbidden HOMO-LUMO transition with an intra-shell nature. The current-density calculations based on the gauge including magnetically induced current method

[*] A. Nishiyama, M. Fukuda, Prof. Dr. H. Furuta, Prof. Dr. S. Shimizu
Department of Chemistry and Biochemistry, Graduate School of Engineering, Kyushu University, Fukuoka 819-0395 (Japan)
E-mail: hfuruta@cstf.kyushu-u.ac.jp, ssoji@cstf.kyushu-u.ac.jp
Dr. S. Mori
Advanced Research Support Center (ADRES), Ehime University Matsuyama 790-8577 (Japan)
Prof. Dr. K. Furukawa
Center for Instrumental Analysis, Institute for Research Promotion, Niigata University, Niigata 950-2181 (Japan)
Dr. H. Fliegl
Hylleraas Centre for Quantum Molecular Sciences, Department of Chemistry, University of Oslo, P.O. Box 1033 Blindern 0315 Oslo (Norway)
E-mail: heike.fliegl@kjemi.uio.no
Prof. Dr. H. Furuta, Prof. Dr. S. Shimizu
Center for Molecular Systems (CMS), Kyushu University, Fukuoka 819-0395 (Japan)

Supporting information and the ORCID identification number(s) for the author(s) of this article is can be found under https://doi.org/10.1002/anie.xxxxxxx .

(GIMIC)[24] also provided quantitative information about the current pathway and the net paratropic ring current of –10.9 nA/T.

At first, we attempted a stepwise synthesis of 5,15-dioxaporphyrin, which involved a hydroxylation reaction of nickel bis(α,α'-dibromodipyrrin) complex **1**[25] with benzaldoxime[26,27] and annulation of the resultant α-hydroxy-substituted species. To our surprise, during the reaction of **1** with benzaldoxime under basic conditions, an intramolecular ether forming reaction of the α-hydroxy-substituted intermediate also took place in a one-pot manner to provide 5,15-dioxaporphyrin **2** (Scheme 1).

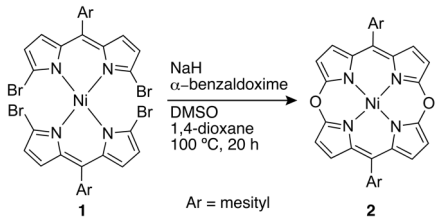

Scheme 1. Synthesis of 5,15-dioxaporphyrin **2**.

The structure of **2** was unambiguously elucidated by X-ray diffraction analysis on crystals obtained from hexane vapor diffusion into a $CHCl_3$ solution of **2** (Figure 1 and Tables S1 and S2). One and half independent structures in the unit cell both exhibited planar structures with small root-mean-square deviations (d_{RMS}) of the π-plane (0.076 and 0.016 Å). The C–O bond lengths of **2** (1.34–1.35 Å) are relatively shorter than a typical C(sp^2)–O single bond (ca. 1.40 Å). An axially pyridine-coordinated crystal structure of **2**, which was obtained when crystals were grown in the presence of excess pyridine, also exhibited a planar structure with d_{RMS} of 0.033 Å (Figure S1 and Tables S2 and S3). These structural features imply that lone-pair electrons of the *meso*-oxygen atoms are successfully incorporated into the π-system of **2**.

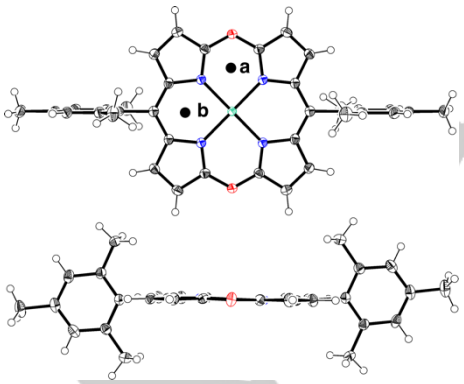

Figure 1. X-ray single crystal structure of **2**, top view (top) and side view (bottom). The thermal ellipsoids are scaled to the 50% probability level. a and b in the top view denote the centers of six-membered rings.

Two doublet signals of the β-pyrrolic protons of **2** at δ = 5.66 and 5.12 ppm were slightly upfield shifted from that of normal pyrrole at δ = 6.2 ppm in $CDCl_3$ due to the paratropic ring current effect arising from the 20π-electron antiaromatic conjugation (Figure S2). The extent of paratropicity of **2** is, however, rather smaller than that of the isoelectronic 5,15-diaza-5,15-dihydroporphyrins,[9,10] the β-pyrrolic protons of which resonated at around 2.8–4.7 ppm. The weaker paratropicity of **2** than 5,15-diaza-5,15-dihydroporphyrins can be generalized in a similar manner in terms of the weaker aromaticity of furan than pyrrole due to greater electronegativity of oxygen than nitrogen, which hampers global delocalization of lone-pair electrons.[28]

In order to gain deeper insight into the weak paratropicity of **2**, a theoretical investigation has also been conducted. Nucleus-independent chemical-shift (NICS(0)) values at "a" and "b" positions in Figure 1 are δ = 6.9 and 8.1 ppm, respectively (Table S4). These rather small positive NICS(0) values compared to those of the nickel complex of 5,15-diaza-5,15-dihydroporphyrins, which exhibits NICS(0) values of δ = 14.5 and 15.5 ppm at the corresponding positions,[10] are consistent with the modest paratropicity observed in the ^{1}H NMR spectrum of **2**. In addition, the negative NICS(0) values at the centers of pyrrole rings (δ = –3.9 ppm) imply non-negligible diatropic contribution of the pyrrole rings (Table S4). We, then, calculated the magnetically induced current density using the GIMIC method, which is a reliable means to determine the degree of aromaticity in a quantitative manner.[24] The present calculations revealed that the ring current of **2** is antiaromatic according to the magnetic criterion with a net current strength of –10.9 nA/T, whereas the outer pyrrolic β-β carbon double bonds serve to produce a local diatropic current of ca. 2.0 nA/T (Figure 2a). The magnetically induced paratropic current preferably flows the inner pathway as highlighted with yellow lines in the streamline visualization (Figure 2b). The current density results provide a reasonable explanation for the experimentally observed modest paratropicity of **2** as well as the reversal of the signs of the NICS(0) values between the inside of the macrocycle and the centers of the pyrrole rings.

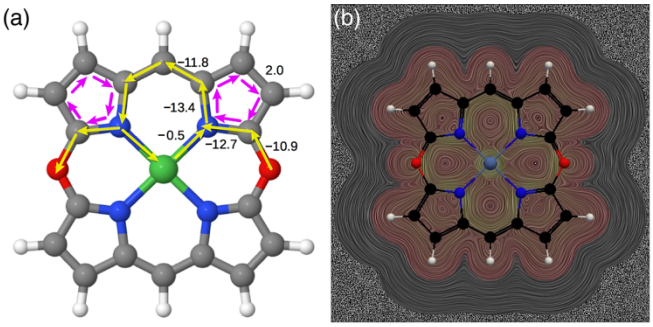

Figure 2. (a) Integrated total current strength susceptibility values obtained for selected bonds are given in nA/T. Diatropic currents are assumed to circle clockwise (magenta arrows), whereas paratropic ones circle in the opposite direction (yellow arrows). (b) Streamline visualization of the magnetically induced current density in a plane placed 1 Bohr below the molecular plane.

In the UV/Vis/NIR absorption spectrum, **2** displayed three characteristic bands at 477, 434, and 329 nm and broad, ill-defined absorption ranging from 600 to 900 nm (Figure 3). This absorption spectral profile, which is characteristic for antiaromatic

conjugated systems,[11-23,29,30] can be explained on the basis of Michl's 4*N*-electron perimeter model[31] with the help of magnetic circular dichroism (MCD) spectroscopy. In Michl's terminology, six frontier orbitals (*h*–, *h*+, *s*–, *s*+, *l*–, *l*+), which are derived from a symmetry perturbation of the degenerate HOMO, singly-occupied molecular orbital (SOMO) and LUMO of the 4*N*-electron perimeter model, mainly contribute to the π-π* transitions, namely S, N (N_1 and N_2), and P (P_1 and P_2) bands. The S band arising from *s*– → *s*+ transition (HOMO → LUMO in the case of **2**) is forbidden due to an intra-shell transition nature. In contrast, the N and P bands can be observed as weak and intense bands because N_1 and P_1 bands and N_2 and P_2 bands are created by configurational interactions of *s*– → *l*– and *h*+ → *s*+ transitions and *s*– → *l*+ and *h*– → *s*+ transitions, respectively. The theoretical absorption of **2** based on TDDFT calculations at the level of B3LYP/SDD for Ni and 6-31G(d) for the remaining atoms is in good agreement with the prediction based on the perimeter model (Table S5). In addition, similar nodal patterns to the 20π-electron [16]annulene ($C_{16}H_{16}^{4-}$) parent hydrocarbon perimeter can be observed for the frontier molecular orbitals (MOs) of **2** (Figure S3). The broad, less-intense absorption of **2** centered at 700 nm can, therefore, be assigned as the S band, whereas the intense bands at 477 and 434 nm mainly comprise the P_1 and P_2 bands, respectively. This assignment was experimentally supported by the MCD spectrum of **2**, which exhibited strongly-coupled Faraday *B* terms with trough and peak at 476 and 434 nm (Figure 3).

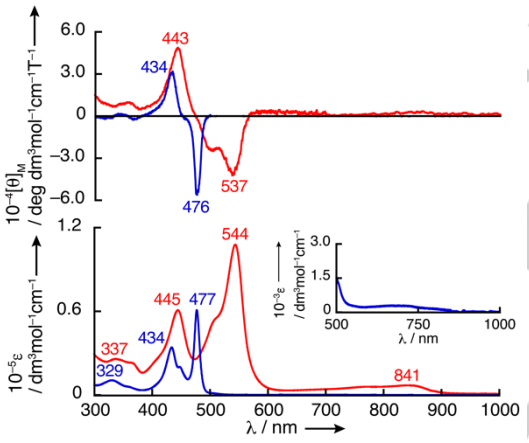

Figure 3. UV/Vis/NIR absorption (bottom) and MCD (top) spectra of **2** (blue line) and **3** (red line) in $CHCl_3$. The inset shows the absorption spectrum of **2** in the Vis/NIR regions.

Electrochemical properties of **2** were investigated by cyclic voltammetry. **2** showed two reversible oxidations at 0.05 and 0.68 V (vs. Fc^+/Fc) and two irreversible reductions at –1.34 and –1.87 V in CH_2Cl_2 (Figure S4), which significantly shifted to the positive compared to the isoelectronic 5,15-diaza-5,15-dihydroporphyrins.[9,10] Since this result inferred stepwise one-electron oxidations from the 20π-electron neutral species to the 19π-electron radical cation and further to the 18π-electron dication, the spectroelectrochemistry measurements were, then, performed (Figure S5). At the first oxidation potential, an NIR band centered at 1168 nm arose. Despite the red-shift, similar NIR band was also observed for the 19π-electron radical species of 5,15-diaza-5,15-dihydroporphyrin.[9] Upon applying higher potentials between the first and second oxidation potentials, another NIR band appeared in the longer wavelength region at 1497 nm. Considering that the overall absorption spectral profile was different from what was expected for a porphyrin-like 18π-electron aromatic system, chemical oxidation of **2** was examined in order to track oxidized species. After oxidation of **2** with $AgPF_6$, MALDI-TOF mass spectrometry revealed generation of dimer and other oligomer species. Among them, the dimer was characterized as β,β-linked compounds based on the ^{1}H NMR spectra and single crystal X-ray diffraction analysis as discussed below. Referring to the Ag^I-promoted *meso-meso* coupling reaction of *meso*-free porphyrin reported by Osuka *et al.*,[32] the oxidation of **2** was, then, examined under various reaction conditions in order to obtain the dimer as a main product. After careful survey of conditions by changing solvents and the amount of $AgPF_6$, β,β-linked dimer **3** was obtained in 33% yield along with recovery of **2** from the reaction with 1.2 equiv of $AgPF_6$ in $CHCl_3$ and acetonitrile (Scheme 2).

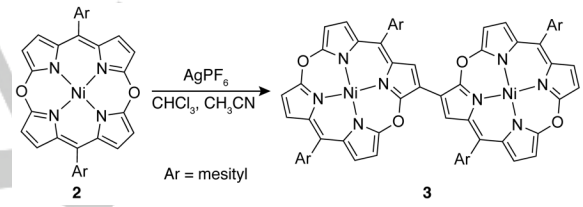

Scheme 2. Synthesis of β,β-linked dimer **3**.

In the ^{1}H NMR spectrum of **3**, the β-pyrrolic protons resonated as six doublets at δ = 5.65, 5.62, 5.56, 5.09, 5.06 and 4.54 ppm and as one singlet at 5.40 ppm, which can be assigned as the β-pyrrolic protons of the β,β-linked pyrrole rings (Figure S6). The up-field shifts of these β-pyrrolic protons indicated that antiaromatic nature of **2** was maintained after dimerization. The X-ray diffraction analysis on **3** revealed the β,β-linking position with C–C bond distance of 1.465(5) Å and co-planar arrangement of the monomer units. There are hydrogen bonding interactions between β-C–H and *meso*-O atoms with a distance of ca. 2.5 Å (Figure 4). Similar parallel arrangement can be seen for a 5,15-diazaporphyrin dimer.[33] These structural features reflect less steric hindrance around the linking position compared to β,β-linked porphyrin dimers.[34,35] The UV/Vis/NIR absorption spectrum of **3** exhibited significant red-shift of the P_1 band by 2580 cm^{-1} from **2**, whereas the shift of the P_2 band was rather small (570 cm^{-1}, Figure 3). Modest intensification of the S band region was also observed upon dimerization.[21a,d] In the case of *meso,meso*-linked and β,β-linked porphyrin dimers, similar absorption spectral changes from the corresponding monomers were explained in terms of the exciton coupling of two perpendicularly arranged transition dipole moments of the Soret bands.[34-36] The perpendicular nature of the transition dipole moments of the P_1 and P_2 bands of **2** based on the TDDFT calculations clearly illustrates stronger exciton coupling of the P_1 band than the P_2 band along the β,β-linking direction (Table S5).

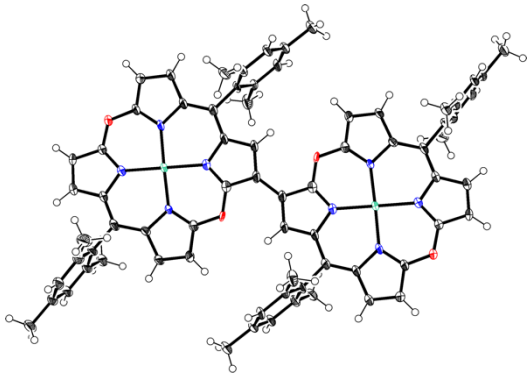

Figure 4. X-ray single crystal structure of **3**. The thermal ellipsoids are scaled to the 50% probability level.

In the cyclic voltammogram, **3** exhibits four oxidations –0.08 0.24, 0.74 and 0.86 V (vs. Fc^+/Fc) and two irreversible reductions at –1.39 and –1.92 V in CH_2Cl_2. Each two of the four oxidations correspond to the first and second oxidations of **2**, which are split into two processes due to electronic interactions between the monomer units (Figure S7). In order to confirm the origin of the broad NIR band at 1497 nm observed in the spectroelectrochemistry of **2**, the UV/Vis/NIR absorption spectrum of **3** was measured upon electrochemical oxidation (Figure S8). By applying the potential above the second oxidation potential of **3**, similar broad NIR band appeared (Figure S8b). The NIR absorption was also observed in a chemical oxidation reaction, in which **3** was added to a CH_2Cl_2 solution containing excess tris(4-bromophenyl)ammoniumyl hexachloroantimonate (Magic Blue, Figure S9). These results indicated that **3** was formed as a dication species during the electrochemical oxidation of **2**.

Finally, in order to reveal the peripheral reactivity of radical cation species of **2**, electrochemical ESR measurement of **2** was performed. Upon oxidation at the first oxidation potential, an ESR signal at g = 2.0018 with hyperfine structure derived from β-protons appeared (Figure S10). This hyperfine structure was also supported by the spin distribution pattern calculated for the radical cation structure of **2** by the DFT method (Figure S11). Delocalization of the radical spin on the β-positions clearly explained the peripheral reactivity towards β,β-linked oligomers.

In summary, 5,15-dioxaporphyrin was rationally synthesized for the first time from the hydroxylation reaction of nickel bis(α,α'-dibromodipyrrin) complex with benzaldoxime followed by intramolecular annulation reaction. The Hückel antiaromatic characteristics of 5,15-dioxaporphyrin arising from the 20π-electron conjugation were revealed by ^{1}H NMR spectroscopy, and its electronic structure was characterized experimentally by UV/Vis/NIR absorption and MCD spectroscopies and theoretically by TDDFT, NICS and GIMIC calculations. 5,15-Dioxaporphyrin is stable under ambient conditions, whereas it forms a β,β-linked dimer upon oxidation instead of attaining 18π-electron aromatic oxidation state. Since it is recently reported that antiaromatic norcorrole exhibit unique conducting properties arising from the small HOMO-LUMO gap[37] and its laminated dimer attains three-dimensional aromaticity,[38] such extension of research on 5,15-dioxaporphyrin is of significant interest, and investigation along these lines is being intensively pursued in our laboratory.

Acknowledgements

This work was supported by Grants-in-Aid for Young Scientists A (JSPS KAKENHI Grant Number JP26708003) and Scientific Research on Innovative Area, "π-System Figuration: Control of Electron and Structural Dynamism for Innovative Functions (No. 2601)" (JSPS KAKENHI Grant Number JP15H01001). H.F. thanks the Norwegian Research Council through the CoE Hylleraas Centre for Quantum Molecular Sciences (Grant Nos. 262695 and 231571/F20) for support. This work has received support from the Norwegian Supercomputing Program (NOTUR) through a grant of computer time (Grant No. NN4654K).

Keywords: Antiaromaticity • Porphyrinoids • Heterocyclic compounds • Redox chemistry • GIMIC

[1] (a) *Heme Biochemistry in Handbook of Porphyrin Science, Vol. 26*, (Eds.: K. M. Kadish, K. M. Smith, R. Guilard), World Scientific, Singapore, **2013**; (b) *Chlorophyll, Photosynthesis and Bio-inspired Energy in Handbook of Porphyrin Science, Vol. 28*, (Eds.: K. M. Kadish, K. M. Smith, R. Guilard), World Scientific, Singapore, **2013**; (c) *Heme Proteins — Part II in Handbook of Porphyrin Science, Vol. 30*, (Eds.: K. M. Kadish, K. M. Smith, R. Guilard), World Scientific, Singapore, **2013**

[2] (a) H. Sato, Y. Higashimoto, H. Sakamoto, M. Sugishima, K. Takahashi, G. Palmer, M. Noguchi, *J. Inorg. Biochem.* **2007**, *101*, 1394-1399; (b) H. Sato, Y. Higashimoto, H. Sakamoto, M. Sugishima, C. Shimokawa, J. Harada, G. Palmer, M. Noguchi, *J. Inorg. Biochem.* **2011**, *105*, 289-296.

[3] A. L. Balch, F. L. Bowles, in *Handbook of Porphyrin Science, Vol. 8* (Eds.: K. M. Kadish, K. M. Smith, R. Guilard), World Scientific, Singapore, **2010**, pp. 293-342.

[4] Y. Matano, *Chem. Rev.* **2016**, *117*, 3138-3191 and references therein.

[5] *Phthalocyanine: Properties and Applications, Vol. 1-4*, (Eds.: C. C. Laznoff, A. B. P. Lever), Wiley-VCH, New York, **1989-1996**.

[6] (a) M. Gouterman, *J. Chem. Phys.* **1959**, *30*, 1139-1161; (b) M. Gouterman, *J. Mol. Spectrosc.* **1961**, *6*, 138-163.

[7] M. J. Broadhurst, R. Grigg, A. W. Johnson, *J. Chem. Soc., Perkin Trans. 1* **1972**, 1124-1135.

[8] H. Kamiya, T. Kondo, T. Sakida, S. Yamaguchi, H. Shinokubo, *Chem. Eur. J.* **2012**, *18*, 16129-16135.

[9] (a) T. Satoh, M. Minoura, H. Nakano, K. Furukawa, Y. Matano, *Angew. Chem.* **2016**, *128*, 2275-2278; *Angew. Chem. Int. Ed.* **2016**, *55*, 2235-2238; (b) K. Sudoh, T. Satoh, T. Amaya, K. Furukawa, M. Minoura, H. Nakano, Y. Matano, *Chem. Eur. J.* **2017**, *23*, 16364-16373.

[10] A. Yamaji, H. Tsurugi, Y. Miyake, K. Mashima, H. Shinokubo, *Chem. Eur. J.* **2016**, *22*, 3956-3961.

[11] (a) E. Vogel, P. Röhrig, M. Sicken, B. Knipp, A. Herrmann, M. Pohl, H. Schmickler, J. Lex, *Angew. Chem.* **1989**, *101*, 1683-1687; *Angew. Chem. Int. Ed. Engl.* **1989**, *28*, 1651-1655; (b) M. Pohl, H. Schmickler, J. Lex, E. Vogel, *Angew. Chem.* **1991**, *103*, 1737-1741; *Angew. Chem. Int. Ed. Engl.* **1991**, *30*, 1693-1697.

[12] G. L. Closs, L. E. Closs, *J. Am. Chem. Soc.* **1963**, *85*, 818-819.

[13] R. Cosmo, C. Kautz, K. Meeholz, J. Heinze, K. Müllen, *Angew. Chem.* **1989**, *101*, 638-640; *Angew. Chem. Int. Ed. Engl.* **1989**, *28*, 604-606.

[14] J.-i. Setsune, K. Kashihara, K.-i. Wada, H. Shiozaki, *Chem. Lett.* **1999**, *28*, 847-848.

[15] (a) B. K. Reddy, A. Basavarajappa, M. D. Ambhore, V. G. Anand, *Chem. Rev.* **2017**, *117*, 3420-3443; (b) J. S. Reddy, V. G. Anand, *J. Am. Chem. Soc.* **2008**, *130*, 3718-3719.

[16] M. Kon-no, J. Mack, N. Kobayashi, M. Suenaga, K. Yoza, T. Shinmyozu, *Chem. Eur. J.* **2012**, 13361-13371.

[17] (a) Y. Matano, T. Nakabuchi, S. Fujishige, H. Nakano, H. Imahori, *J. Am. Chem. Soc.* **2008**, *130*, 16446-16447; (b) T. Nakabuchi, M. Nakashima, S. Fujishige, H. Nakano, Y. Matano, H. Imahori, *J. Org. Chem.* **2010**, *75*, 375-389.

[18] (a) J. A. Cissell, T. P. Vaid, A. L. Rheingold, *J. Am. Chem. Soc.* **2005**, *127*, 12212-12213; (b) J. A. Cissell, T. P. Vaid, G. P. A. Yap, *J. Am. Chem. Soc.* **2007**, *129*, 7841-7847.

[19] M. Bröring, S. Köhler, C. Kleeberg, *Angew. Chem.* **2008**, *120*, 5740-5743; *Angew. Chem. Int. Ed.* **2008**, *47*, 5658-5660.

[20] (a) T. Ito, Y. Hayashi, S. Shimizu, J.-Y. Shin, N. Kobayashi, H. Shinokubo, *Angew. Chem.* **2012**, *124*, 8670-8673; *Angew. Chem. Int. Ed.* **2012**, *51*, 8542-8545; (b) J.-Y. Shin, T. Yamada, H. Yoshikawa, K. Awaga, H. Shinokubo, *Angew. Chem.* **2014**, *126*, 3160-3165; *Angew. Chem. Int. Ed.* **2014**, *53*, 3096-3101; (c) T. Fukuoka, K. Uchida, Y. M. Sung, J.-Y. Shin, S. Ishida, J. M. Lim, S. Hiroto, K. Furukawa, D. Kim, T. Iwamoto, H. Shinokubo, *Angew. Chem.* **2014**, *126*, 1532-1535; *Angew. Chem. Int. Ed.* **2014**, *53*, 1506-1509; (d) R. Nozawa, K. Yamamoto, J.-Y. Shin, S. Hiroto, H. Shinokubo, *Angew. Chem.* **2015**, *127*, 8474-8577; *Angew. Chem. Int. Ed.* **2015**, *54*, 8454-8457; (e) R. Nozawa, K. Yamamoto, I. Hisaki, J.-Y. Shin, H. Shinokubo, *Chem. Commun.* **2016**, *52*, 7106-7109; (f) T. Yoshida, D. Sakamaki, S. Seki, H. Shinokubo, *Chem. Commun.* **2017**, *53*, 1112-1115; (g) T. Yonezawa, S. A. Shafie, S. Hiroto, H. Shinokubo, *Angew. Chem.* **2017**, *129*, 11984-11987; *Angew. Chem. Int. Ed.* **2017**, *56*, 11822-11825 (h) T. Yoshida, K. Takahashi, Y. Ide, R. Kishi, J.-y. Fujiyoshi, S. Lee, Y. Hiraoka, D. Kim, M. Nakano, T. Ikeue, H. Yamada, H. Shinokubo, *Angew. Chem.* **2018**, *130*, 2231-2235; *Angew. Chem. Int. Ed.* **2018**, *57*, 2209-2213.

[21] (a) B. Liu, X. Li, M. Stępień, P. J. Chmielewski, *Chem. Eur. J.* **2015**, *21*, 7790-7797; (b) Z. Deng, X. Li, M. Stępień, P. J. Chmielewski, *Chem. Eur. J.* **2016**, *22*, 4231-4246; (c) B. Liu, T. Yoshida, X. Li, M. Stępień, H. Shinokubo, P. J. Chmielewski, *Angew. Chem.* **2016**, *128*, 13336-13340; *Angew. Chem. Int. Ed.* **2016**, *55*, 13142-13146; (d) X. Li, Y. Meng, P. Yi, M. Stępień, P. J. Chmielewski, *Angew. Chem.* **2017**, *129*, 10950-10954; *Angew. Chem. Int. Ed.* **2017**, *56*, 10810-10814.

[22] (a) J. L. Sessler, S. J. Weghorn, T. Morishima, M. Rosingana, V. Lynch, V. Lee, *J. Am. Chem. Soc.* **1992**, *114*, 8306-8307; (b) J. L. Sessler, D. Seidel, *Angew. Chem.* **2003**, *115*, 5292-5333; *Angew. Chem. Int. Ed.* **2003**, *42*, 5134-5175 and references therein.

[23] (a) S. Saito, A. Osuka, *Angew. Chem.* **2011**, *123*, 4432-4464; *Angew. Chem. Int. Ed.* **2011**, *50*, 4342-4373; (b) T. Tanaka, A. Osuka, *Chem. Rev.* **2017**, *117*, 2584-2640 and references therein.

[24] (a) R. R. Valiev, I. Benkyi, Y. V. Konyshev, H. Fliegl, D. Sundholm, *J. Phys. Chem. A* **2018**, *122*, 4756-4767; (b) H. Fliegl, R. R. Valiev, F. Pichierri, D. Sundholm, *Chem. Modell.* **2018**, *14*, 1-42; (c) D. Sundholm, H. Fliegl, R. J. F. Berger, *WIREs Comput. Mol. Sci.* **2016**, 1-40; (d) I. Benkyi, H. Fliegl, R. R. Valiev, D. Sundholm, *Phys. Chem. Chem. Phys.* **2016**, *18*, 11932-11941; (e) H. Fliegl, J. Jusélius, D. Sundholm, *J. Phys. Chem. A* **2016**, *120*, 5658-5664; (f) H. Fliegl, S. Taubert, O. Lehtonen, D. Sundholm, *Phys. Chem. Chem. Phys.* **2011**, *13*, 20500-20518; (g) J. Jusélius, D. Sundholm, J. Gauss, *J. Chem. Phys.* **2004**, *121*, 3952-3963.

[25] Y. Matano, T. Shibano, H. Nakano, H. Imahori, *Chem. Eur. J.* **2012**, *18*, 6208-6216.

[26] (a) M. J. Crossley, L. G. King, S. M. Pyke, *Tetrahedron* **1987**, *43*, 4569-4577; (b) M. J. Crossley, P. L. Burn, S. J. Langford, S. M. Pyke, A. G. Stark, *J. Chem. Soc., Chem. Commun.* **1991**, 1567-1568.

[27] K. Yoshida, W. Cha, D. Kim, A. Osuka, *Angew. Chem.* **2017**, *129*, 2532-2536; *Angew. Chem. Int. Ed.* **2017**, *56*, 2492-2496.

[28] C. Kumar, H. Fliegl, D. Sundholm, *J. Phys. Chem. A*, **2017**, *121*, 7282-7289.

[29] (a) A. Muranaka, O. Matsushita, K. Yoshida, S. Mori, M. Suzuki, T. Furuyama, M. Uchiyama, A. Osuka, N. Kobayashi, *Chem. Eur. J.* **2009**, *15*, 3744-3751; (b) T. Furuyama, T. Sato, N. Kobayashi, *J. Am. Chem. Soc.* **2015**, *137*, 13788-13791.

[30] M. Ishida, T. Furuyama, J. M. Lim, S. Lee, Z. Zhang, S. K. Ghosh, V. M. Lynch, C.-H. Lee, N. Kobayashi, D. Kim, J. L. Sessler, *Chem. Eur. J.* **2017**, *23*, 6682-6692.

[31] (a) J. Fleischhauer, U. Höweler, J. Michl, *J. Phys. Chem. A* **2000**, *104*, 7762-7775; (b) J. Fleischhauer, U. Höweler, J. Spanget-Larsen, G. Raabe, J. Michl, *J. Phys. Chem. A* **2004**, *108*, 3225-3234; (c) U. Howeler, J. W. Downing, J. Fleischhauer, J. Michl, *J. Chem. Soc., Perkin. Trans. 2* **1998**, 1101-1118.

[32] (a) A. Osuka, H. Shimidzu, *Angew. Chem.* **1997**, *109*, 93-95; *Angew. Chem. Int. Ed. Engl.* **1997**, *36*, 135-137; (b) N. Aratani, A. Osuka, Y. H. Kim, D. H. Jeong, D. Kim, *Angew. Chem.* **2000**, *112*, 1517-1521; *Angew. Chem. Int. Ed.* **2000**, *39*, 1458-1462.

[33] Y. Matano, D. Fujii, T. Shibano, K. Furukawa, T. Higashino, H. Nakano, H. Imahori, *Chem. Eur. J.* **2014**, *20*, 3342-3349.

[34] (a) Y. Deng, C. K. Chang, D. G. Nocera, *Angew. Chem.* **2000**, *112*, 1108-1110; *Angew. Chem. Int. Ed.* **2000**, *39*, 1066-1068; (b) H. Uno, Y. Kitawaki, N. Ono, *Chem. Commun.* **2002**, 116-117; (c) H. Hata, H. Shinokubo, A. Osuka, *J. Am. Chem. Soc.* **2005**, *127*, 8264-8265.

[35] G. Bringmann, D. C. G. Götz, T. A. M. Gulder, T. H. Gehrke, T. Bruhn, T. Kupfer, K. Radacki, H. Braunschweig, A. Heckmann, C. Lambert, *J. Am. Chem. Soc.* **2008**, *130*, 17812-17825.

[36] S. Cho, M.-C. Yoon, J. M. Lim, P. Kim, N. Aratani, Y. Nakamura, T. Ikeda, A. Osuka, D. Kim, *J. Phys. Chem. B* **2009**, *113*, 10619-10627.

[37] S. Fujii, S. Marqué-González, J.-Y. Shin, S. Hiroshi, T. Matsuda, T. Nishino, A. Narendra P, H. Vázquez, M. Kiguchi, *Nat. Commun.* **2017**, *8*, 15984.

[38] R. Nozawa, H. Tanaka, W.-Y. Cha, Y. Hong, I. Hisaki, S. Shimizu, J.-Y. Shin, S. Irle, T. Kowalczyk, D. Kim, H. Shinokubo, *Nat. Commun.* **2016**, *7*, 13620.

Entry for the Table of Contents

COMMUNICATION

5,15-Dioxaporphyrin was synthesized for the first time, and its antiaromatic optical and electrochemical properties arising from the 20π-electron conjugated system were revealed. In addition, this unprecedented molecule exhibits unique reactivity to form the β,β-linked dimer upon oxidation.

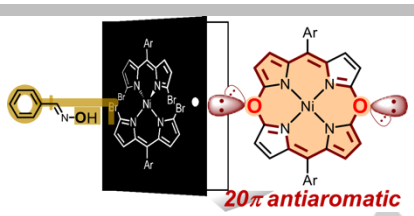

A. Nishiyama, M. Fukuda, S. Mori, K. Furukawa, H. Fliegl, H. Furuta,* S. Shimizu**

Page No. – Page No.

First Rational Synthesis of Antiaromatic 5,15-Dioxaporphyrin and Its β,β-Linked Dimer Formation upon Oxidation